J|A|C|S
ARTICLES
Published on Web 03/25/2005

Structure, Function, and Inhibition along the Reaction Coordinate of CTX-M β-Lactamases

Yu Chen,[†] Brian Shoichet,*[,†] and Richard Bonnet*[,†,‡]

Contribution from the Department of Pharmaceutical Chemistry, University of California, San Francisco, Genentech Hall, 600 16th Street, San Francisco, California 94143-2240, and Laboratoire de Bactériologie, Centre Hospitalier Universitaire − Faculté de Médecine, 28 Place Henri-Dunant, 63001 Clermont-Ferrand Cedex, France

Received November 27, 2004; E-mail: shoichet@cgl.ucsf.edu; Richard.Bonnet@u-clermont1.fr

Abstract: CTX-M enzymes are an emerging group of extended spectrum β-lactamases (ESBLs) that hydrolyze not only the penicillins but also the first-, second-, and third-generation cephalosporins. Although they have become the most frequently observed ESBLs in certain areas, there are few effective inhibitors and relatively little is known about their detailed mechanism. Here we describe the X-ray crystal structures of CTX-M enzymes in complex with different transition-state analogues and β-lactam inhibitors, representing the enzyme as it progresses from its acylation transition state to its acyl enzyme complex to the deacylation transition state. As the enzyme moves along this reaction coordinate, two key catalytic residues, Lys73 and Glu166, change conformations, tracking the state of the reaction. Unexpectedly, the acyl enzyme complex with the β-lactam inhibitor cefoxitin still has the catalytic water bound; this water had been predicted to be displaced by the unusual 7α-methoxy of the inhibitor. Instead, the 7α-group appears to inhibit by preventing the formation of the deacylation transition state through steric hindrance. From an inhibitor design standpoint, we note that the best of the reversible inhibitors, a ceftazidime-like boronic acid compound, binds to CTX-M-16 with a K_i value of 4 nM. When used together in cell culture, this inhibitor reversed cefotaxime resistance in CTX-M-producing bacteria. The structure of its complex with CTX-M enzyme and the structural view of the reaction coordinate described here provide templates for inhibitor design and intervention to combat this family of antibiotic resistance enzymes.

Introduction

The expression of β-lactamases is the most common cause of resistance to the β-lactam antibiotics, such as penicillins and cephalosporins.[1] Of the four classes of β-lactamases, class A, C, and D enzymes use a catalytic serine to hydrolyze the β-lactam ring and class B enzymes use a metal cofactor. Class A enzymes are most frequently encountered in clinical isolates.

To combat class A β-lactamases, "β-lactamase-stable" compounds were introduced, subsequently followed by β-lactamase inhibitors. Both types of compounds preserve the β-lactam core and the C3(4)′ carboxylate of the drug but explore diverse functionalities of the R1 side chain on the C6(7) position of the penicillin/cephalosporin ring (Figure 1). The different R1 side chains confer different pharmacological profiles, bacterial spectra of action, and different levels of resistance to β-lactamases. Whereas early β-lactam antibiotics, such as penicillins and first-generation cephalosporins, are rapidly inactivated by β-lactamases, later agents such as third-generation cephalosporins (cefotaxime and ceftazidime) and cefoxitin (Figure 1) are relatively inert to or indeed inhibit these enzymes.

In response to these new drugs, class A extended-spectrum β-lactamases (ESBLs) and inhibitor-resistant enzymes appeared,[2,3] leading to major treatment problems in many clinical settings, particularly in intensive care units. First observed in 1983, the class A ESBLs and class A inhibitor-resistant enzymes were derived from the well-known penicillinases TEM-1, TEM-2, and SHV-1 by typically one to four point mutations, which either extended their hydrolytic spectrum to third-generation cephalosporins or conferred resistance to the β-lactamase inhibitors.

Since 1995, a new group of class A ESBLs, called CTX-M enzymes, have emerged worldwide and are now the most frequently observed ESBLs in several areas. CTX-M enzymes share less than 40% identity with TEM- and SHV-type enzymes and form a more heterogeneous ESBL family of 40 members.[4] As their extended spectrum status suggests, they hydrolyze the penicillins and the first-, second-, and third-generation cephalosporins. They differ from most of TEM and SHV ESBLs by

[†] University of California, San Francisco.
[‡] Centre Hospitalier Universitaire − Faculté de Médecine.

(1) Matagne, A.; Dubus, A.; Galleni, M.; Frere, J. M. The beta-lactamase cycle: a tale of selective pressure and bacterial ingenuity. *Nat. Prod. Rep.* **1999**, *16* (1), 1−19.
(2) Bradford, P. A. Extended-spectrum beta-lactamases in the 21st century: characterization, epidemiology, and detection of this important resistance threat. *Clin. Microbiol. Rev.* **2001**, *14* (4), 933−51.
(3) Chaibi, E. B.; Farzaneh, S.; Morand, A.; Peduzzi, J.; Barthelemy, M.; Sirot, D.; Labia, R. Problems encountered in the characterization of IRT beta-lactamase-producing clinical *Escherichia coli* isolates intermediate-resistant to cephalothin. *J. Antimicrob. Chemother.* **1996**, *37* (1), 190−1.
(4) Bonnet, R. Growing group of extended-spectrum beta-lactamases: the CTX-M enzymes. *Antimicrob. Agents Chemother.* **2004**, *48* (1), 1−14.

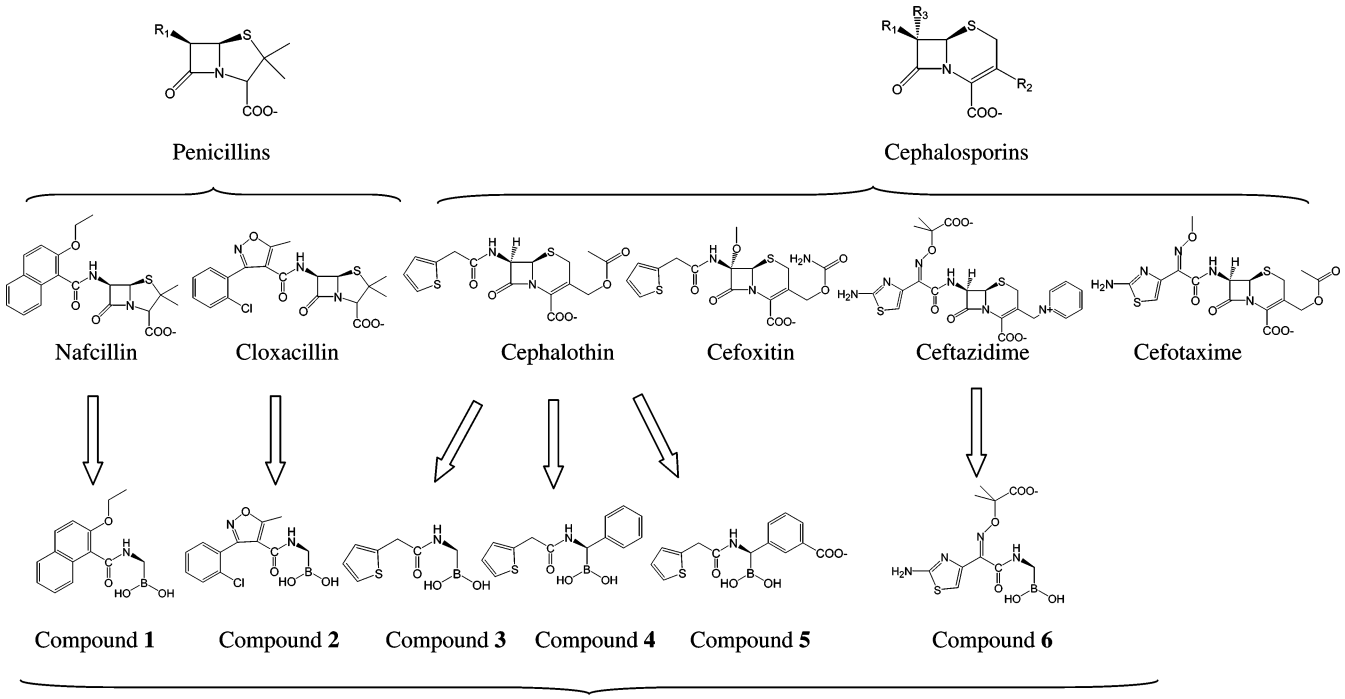

Figure 1. Characteristic β-lactam antibiotics and related β-lactamase inhibitors.

a much greater hydrolytic activity against cefotaxime than against ceftazidime and a different susceptibility profile to inhibitors.

Unlike the well-studied TEM and SHV β-lactamases,[5−8] there have been few biophysical or structural studies of the CTX-M family. An important step was the determination of the X-ray structure of Toho-1, a CTX-M-type enzyme, both in its apo- and β-lactam acyl-intermediate, which significantly advanced our understanding of specific recognition by these enzymes.[9−11] A surprising feature of the Toho-1 structure was that its active site did not feature the enlarged sites characteristic of TEM ESBL mutants such as TEM-52[12] and TEM-64.[7] In these TEM-derived ESBLs, an enlarged active site is thought to be key to their ability to recognize the relatively large third-generation cephalosporins.

Toho-1 is part of an unusual subclass of the CTX-M family, and it was unclear whether this relatively small active site was characteristic of the 40 or more enzymes that make up the CTX-M family. Very recently, however, we determined the structures of CTX-M-9, -14, -16, and -27 and found that these enzymes also have small active sites,[13] suggesting that the earlier Toho structures are characteristic of the class. With apo- and acyl-enzyme complexes of the CTX-M family determined, we now turn our attention to enzyme and substrate structural changes along the reaction coordinate and how an understanding of this coordinate might be exploited for inhibitor discovery. We investigate recognition of two classes of boronic acids and of the β-lactam cefoxitin, each of which is known to inhibit classical class A β-lactamases, such as TEM-1. Glycylboronic acids bearing the R1 side chains of cephalosporins and penicillins, such as compounds **1** and **2** (Figure 1), bind to the class A β-lactamase TEM-1 as acylation transition-state analogues (step 2, Figure 2). Chiral glycylboronic acids, such as compound **5** (Figure 1), bind to TEM as deacylation transition state analogues (step 4, Figure 2). These boronic acids are especially useful for probing recognition in that they are reversible inhibitors, forming fast-on/fast-off Lewis acid adducts with serine β-lactamases, allowing K_i values to be converted into thermodynamic binding affinities. Cefoxitin, on the other hand, is an irreversible inhibitor of class A β-lactamases, but its enzyme adduct is long-lived enough to probe using reversible enzyme denaturation, which also may be interpreted thermodynamically.[7,14−16]

(5) Knowles, J. R. Penicillin resistance: the chemistry of β-lactamase inhibition. **1985**, *18* (4), 97−104.
(6) Massova, I.; Mobashery, S. Structural and mechanistic aspects of evolution of beta-lactamases and penicillin-binding proteins. *Curr. Pharm. Des.* **1999**, *5* (11), 929−37.
(7) Wang, X.; Minasov, G.; Shoichet, B. K., Evolution of an antibiotic resistance enzyme constrained by stability and activity tradeoffs. *J. Mol. Biol.* **2002**, *320* (1), 85−95.
(8) Nukaga, M.; Mayama, K.; Hujer, A. M.; Bonomo, R. A.; Knox, J. R. Ultrahigh-resolution structure of a class A beta-lactamase: on the mechanism and specificity of the extended-spectrum SHV-2 enzyme. *J. Mol. Biol.* **2003**, *328* (1), 289−301.
(9) Shimamura, T.; Ibuka, A.; Fushinobu, S.; Wakagi, T.; Ishiguro, M.; Ishii, Y.; Matsuzawa, H., Acyl-intermediate structures of the extended-spectrum class A beta-lactamase, Toho-1, in complex with cefotaxime, cephalothin, and benzylpenicillin. *J. Biol. Chem.* **2002**, *277* (48), 46601−8.
(10) Ibuka, A. S.; Ishii, Y.; Galleni, M.; Ishiguro, M.; Yamaguchi, K.; Frere, J. M.; Matsuzawa, H.; Sakai, H. Crystal structure of extended-spectrum beta-lactamase Toho-1: insights into the molecular mechanism for catalytic reaction and substrate specificity expansion. *Biochemistry* **2003**, *42* (36), 10634−43.
(11) Ibuka, A.; Taguchi, A.; Ishiguro, M.; Fushinobu, S.; Ishii, Y.; Kamitori, S.; Okuyama, K.; Yamaguchi, K.; Konno, M.; Matsuzawa, H. Crystal structure of the E166A mutant of extended-spectrum beta-lactamase Toho-1 at 1.8 A resolution. *J. Mol. Biol.* **1999**, *285* (5), 2079−87.
(12) Orencia, M. C.; Yoon, J. S.; Ness, J. E.; Stemmer, W. P.; Stevens, R. C. Predicting the emergence of antibiotic resistance by directed evolution and structural analysis. *Nat. Struct. Biol.* **2001**, *8* (3), 238−42.
(13) Chen, Y.; Delmas, J.; Sirot, J.; Shoichet, B.; Bonnet, R. Atomic resolution structures of CTX-M beta-lactamases: extended spectrum activities from increased mobility and decreased stability. *J. Mol. Biol.* **2005**. In press.
(14) Beadle, B. M.; McGovern, S. L.; Patera, A.; Shoichet, B. K. Functional analyses of AmpC beta-lactamase through differential stability. *Protein Sci.* **1999**, *8* (9), 1816−24.
(15) Nagarajan, R.; Pratt, R. F. Thermodynamic evaluation of a covalently bonded transition state analogue inhibitor: inhibition of beta-lactamases by phosphonates. *Biochemistry* **2004**, *43* (30), 9664−73.

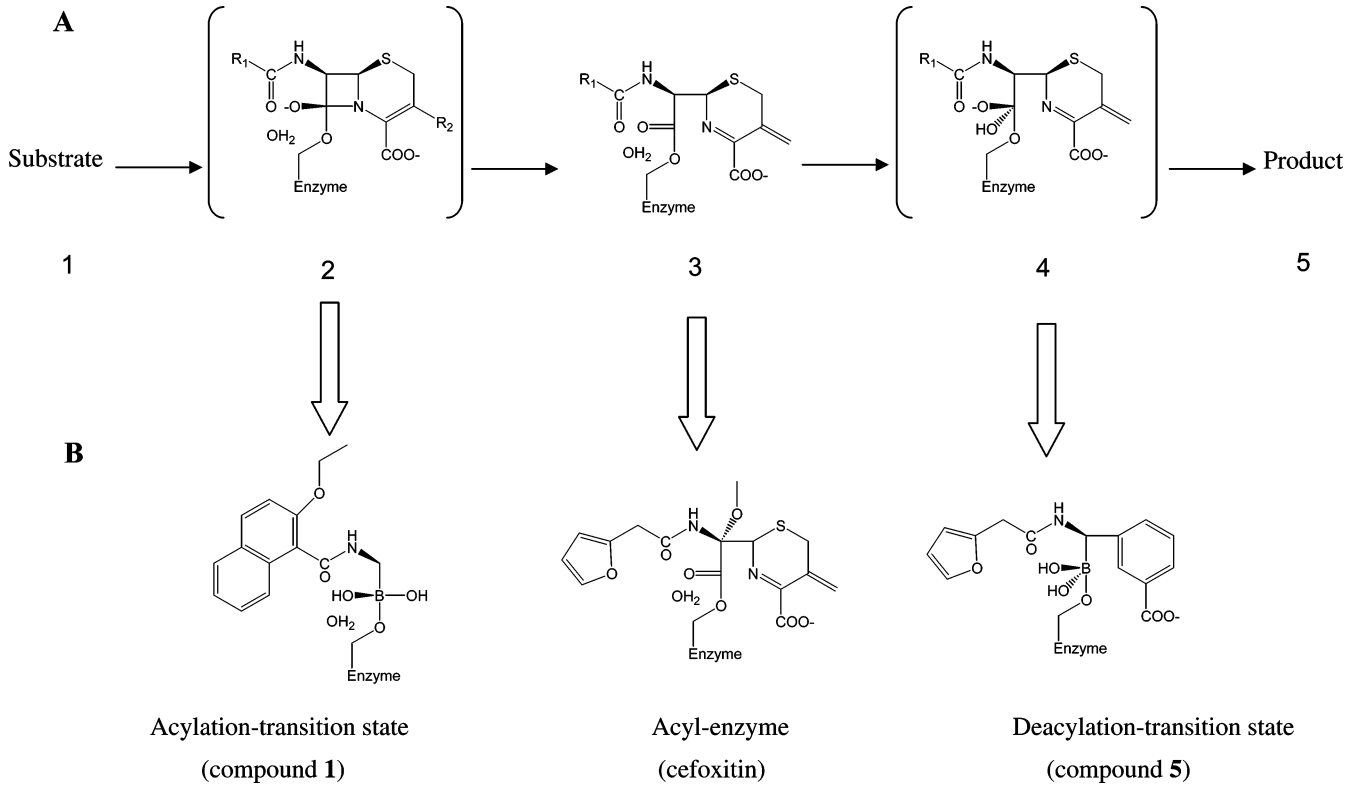

Figure 2. Reaction cycle of a serine β-lactamase. (A) The basic reaction pathway is shown with the acylation and deacylation tetrahedral intermediate. (B) Structural diagrams of the reaction intermediates whose structures have been determined to understand each step.

Here we determine the X-ray structures of the complexes with two glycylboronic acids, the β-lactam inhibitor cefoxitin, and a chiral glycylboronic acid, with two characteristic cefotaximases of the family, CTX-M-9 and CTX-M-14, thereby capturing the enzyme in a state resembling an acylation transition state, the acyl-enzyme intermediate, and a deacylation transition state, respectively. The structures, determined to between 1.16 and 1.7 Å resolution, reveal conformational changes that active site residues undergo along the reaction coordinate. The structures explain why cefoxitin, the β-lactam inhibitor, actually destabilizes the enzyme in its acyl-adduct form and suggest a surprising mechanism of inhibition for this entire class of inhibitors. They also explain the high potency of several of the boronic acids, the most active of which inhibits CTX-M-16 with a K_i of 4 nM. The activity of these compounds at reversing antibiotic resistance is further explored in cell culture.

Materials and Methods

Enzyme Expression and Purification. The CTX-M-encoding gene was cloned by PCR into a modified pET-9a plasmid (Stratagene) to construct a vector for overexpression and sequenced as described.[17] The *E. coli* expression strain BL21 (DE3) (Novagen) was transformed with the pET-bla_{CTX-M} construct. Single colonies of *E. coli* were used to inoculate 3 mL of 2xYT medium (Bio 101, Inc.) containing kanamycin (20 mg/mL) for overnight growth at 37 °C. From this preculture mixture, 8 mL was added to 1L of 2xYT medium in 1-L Erlenmeyer flasks containing kanamycin (20 mg/mL) for aerobic growth at 37 °C under 250-rpm agitation up to an $A_{600\ nm}$ of 0.8. Expression was induced with 0.1 mM isopropyl-*b*-D-thiogalactopyranoside (Sigma), and the cells were grown overnight at 30 °C. Bacteria were collected by centrifugation and harvested with 50 mM MES−NaOH (pH 6.0). The cell pellet was disrupted by one cycle of freezing and thawing, followed by sonication. After centrifugation (13 000 × *g* for 10 min and 48 000 × *g* for 60 min at 4 °C), the clarified supernatant was loaded onto a CM-Fast Flow column (100 mL; Amersham Pharmacia Biotech.) equilibrated with MES−NaOH 50 mM (pH 6.0). Proteins were eluted with a linear NaCl gradient (0 to 150 mM). The β-lactamase-containing elution peak was extensively dialyzed and concentrated by ultrafiltration against 5 mM Tris-HCl buffer (pH 7.0) and concentrated to 20 mg/mL for crystallization. The protein concentration was estimated by the Bio-Rad protein assay (Bio-Rad, Richmond, Calif.), with bovine serum albumin (Sigma) used as a standard. Homogeneity was estimated to be more than 95% by sodium dodecyl sulfate-polyacrylamide gel electrophoresis.

Inhibitors. The glycylboronic acids were synthesized as previously described.[18,19] Cefoxitin was purchased from Sigma and used without further purification.

Enzymology. The glycylboronic acids were dissolved in DMSO stock solutions at 50 mM; more dilute stocks were subsequently prepared as necessary. Enzymes were diluted from stock solutions to a final concentration of 1.5 nM. The enzyme assay was carried out in 50 mM potassium phosphate (pH 7.0) at room temperature and monitored in an HP8453 UV−vis spectrophotometer as previously described.[18,19] Inhibitor and enzyme were incubated together briefly at their final concentration before the reaction was initiated by the addition of 100 μM substrate. K_i values were obtained by comparison of progress curves in the presence and absence of inhibitor, using the method

(16) Rahil, J.; Pratt, R. F. Characterization of Covalently Bound Enzyme Inhibitors as Transition-State Analogues by Protein Stability Measurements: Phosphonate Monoester Inhibitors of a beta-lactamase. *Biochemistry* **1994**, *33*, 116−125.
(17) Bonnet, R.; Sampaio, J. L.; Chanal, C.; Sirot, D.; De Champs, C.; Viallard, J. L.; Labia, R.; Sirot, J. A novel class A extended-spectrum beta-lactamase (BES-1) in *Serratia marcescens* isolated in Brazil. *Antimicrob. Agents Chemother.* **2000**, *44* (11), 3061−8.
(18) Caselli, E.; Powers, R. A.; Blasczcak, L. C.; Wu, C. Y.; Prati, F.; Shoichet, B. K. Energetic, structural, and antimicrobial analyses of beta-lactam side chain recognition by beta-lactamases. *Chem. Biol.* **2001**, *8* (1), 17−31.
(19) Morandi, F.; Caselli, E.; Morandi, S.; Focia, P. J.; Blazquez, J.; Shoichet, B. K.; Prati, F. Nanomolar inhibitors of AmpC beta-lactamase. *J. Am. Chem. Soc.* **2003**, *125* (3), 685−95.

described by Waley.[20] In all reactions, rates were measured after they had overcome their initial lag phase in the cases where this was significant and had reached a steady state. Typically, initial rate fits to the absorbance data for the first 100 s were used to determine reaction velocities. The reaction was monitored at 340 nm using 6-β-furylacryloylamido-penicillanic acid (FAP, Calbiochem) as substrate (the K_m values for CTX-M-9 and CTX-M-16 were 17 μM and 6.5 μM, respectively). The progress curves were measured at least three times for each substrate.

Crystallization. Cocrystals of the CTX-M enzymes in complex with the glycylboronic acids were grown by vapor diffusion in hanging drops equilibrated over 1.4 M potassium phosphate buffer (pH 8.8) using microseeding techniques. To a solution of 10 mg/mL protein in 5mM Tris (pH7.0) and 30mM NaCl was added an equal volume of 2mM inhibitor in a solution of 5% DMSO, 1.25 M potassium phosphate (pH 8.8). Crystals appeared in 8−48 h after equilibration at 20 °C. The cefoxitin complex of CTX-M-9 was obtained by soaking apo-enzyme crystals with 25 mM cefoxitin in 1.4 M potassium phosphate buffer (pH 8.8) overnight at 20 °C. Before data collection, crystals were immersed in a cryoprotectant solution of 30% sucrose, 1.8 M potassium phosphate (pH 8.8), for about 30 s, and were flash frozen in liquid nitrogen.

Data Collection and Structure Determination. Data were measured at 100 K using a ADSC-CCD detector on Beamline 8.3.1 of the Advanced Light Source at Lawrence Berkley National Laboratory. Reflections were indexed, integrated, and scaled using the HKL software package.[21] For all structures, the space group was $P2_1$, with two molecules in the asymmetric unit. Phases were calculated by molecular replacement with the program EPMR[22] using the apo-enzyme structure of CTX-M-9, with water molecules and ions removed.[13] The complex structures of CTX-M-9 and CTX-M-14 with compound **6** at 1.35 Å resolution and CTX-M-9 with compound **5** at 1.16 Å resolution were refined in SHELX97.[23] The refinement was carried out using ADPs (anisotropic displacement parameters) with standard DELU (rigid-bond), SIMU (spatially adjacent atoms), and ISOR (isolated atoms to be approximately isotropic) restraints. DELU, SIMU, and ISOR restraints were adjusted using the program PARVATI.[24] For the other complexes, the models were refined using the maximum likelihood method in CNS including simulated annealing with an initial temperature of 2000 K, positional minimization, and individual B-factor refinement, with a bulk solvent correction.[25] Sigma A-weighted electron density maps were calculated using CNS or SHELX and used in the steps of manual model rebuilding with the program XtalView[26] or ONO.[27] Cross-validation was employed throughout, and 5% of the data were used for the R_{free} calculation. The stereochemical quality of the models was monitored periodically with the program Procheck[28] and RAMPAGE.[29] The figures were generated by Chimera,[30] PyMol (Delano Scientific), and Raster3D.[31]

Thermal Denaturation of CTX-M-9 in Complex with Cefoxitin. Thermal denaturation was carried out in 38% ethylene glycol, 200 mM KCl, 50 mM potassium phosphate at pH 7.0. As previously observed, all melts were over 95% reversible and appeared to be two-state.[13] The cefoxitin adduct with CTX-M-9 was formed by mixing an enzyme solution in a buffer with a 350-fold molar excess of the compound at room temperature. The enzyme or enzyme adduct was denatured by raising the temperature in 0.1 °C increments at a ramp rate of 2 °C/min. Denaturation was marked by an obvious transition in fluorescence signals, which was monitored using an excitation wavelength of 285 nm, a 300-nm cut-out filter, and an integrated emission above 300 nm. A Jasco J-715 spectropolarimeter with a fluorescence attachment, a Peltier-effect temperature controller, and an in-cell temperature monitor was used in these experiments. Each denaturation experiment was performed in triplicate. The melting temperature and van't Hoff enthalpy of unfolding were calculated with EXAM.[32] Changes in unfolding free energy ($\Delta\Delta G_u$) were computed from ΔT_m measurements by the method of Schellman using the unfolding T_m value of the apo-enzyme as reference: $\Delta\Delta G_u = \Delta T_m \Delta S_u^{CTX-M-9}$.[33] A decrease in T_m and a negative $\Delta\Delta G_u$ value indicate destabilization of the adduct relative to the apo-enzyme.

Microbiology. The inhibitors were tested for synergy with the β-lactam ceftazidime against clinical isolates of pathogenic *Escherichia coli*.[34] These bacteria were resistant to β-lactams because of the expression of either CTX-M-9 or CTX-M-16 β-lactamase. Disk diffusion plate assays were performed as follows. Bacterial strains were grown to log-phase and then diluted in sterile water to a turbidity equivalent to 0.5 McFarland turbidity standards. After a 10-fold dilution, the bacterial suspensions were inoculated by swabbing on Muller−Hinton agar medium. The plates were dried for 20 min before applying the disks containing cefotaxime antibiotic or the inhibitor (64 μg) or both. After overnight incubation at 37 °C, the zones of bacterial-growth inhibition were measured. Minimum inhibitor concentration (MIC) values were determined with Mueller−Hinton Broth II using the microdilution method according to NCCLS guidelines.[35] The molar ratio of inhibitor/cefotaxime was one. Each value reported reflects the average of three independent experiments.

Data Deposition. The coordinates and structure factors have been deposited in the Protein Data Bank. The access codes for the complexes are: **6**/CTX-M-9, 1YLY; **6**/CTX-M-14, 1YLZ; **5**/CTX-M-9, 1YM1; **1**/CTX-M-9, 1YMS; cefoxitin/CTX-M-9, 1YMX.

Results

Enzyme Inhibition. All inhibitors acted competitively through formation of a reversible covalent adduct. Whereas most did not have a significant incubation effect, one, compound **5**, did. The IC_{50} for **5** decreased (improved) 2.3-fold on five minute

(20) Waley, S. G. A quick method for the determination of inhibition constants. *Biochem. J.* **1982**, *205* (3), 631−3.
(21) Otwinowski, Z.; Minor, W. Processing of X-ray diffraction data collected in oscillation mode. *Methods Enzymol.* **1997**, *276*, 307−326.
(22) Kissinger, C. R.; Gehlhaar, D. K.; Fogel, D. B. Rapid automated molecular replacement by evolutionary search. *Acta. Crystallogr., Sect. D* **1999**, *55* (Pt 2), 484−91.
(23) Sheldrick, G. M.; Schneider, T. R. SHELXL: High-resolution refinement. *Methods Enzymol.* **1997**, *277*, 319−343.
(24) Merritt, E. A. Expanding the model: anisotropic displacement parameters in protein structure refinement. *Acta Crystallogr., Sect. D* **1999**, 55 (6), 1109−1117.
(25) Brunger, A. T.; Adams, P. D.; Clore, G. M.; DeLano, W. L.; Gros, P.; Grosse-Kunstleve, R. W.; Jiang, J. S.; Kuszewski, J.; Nilges, M.; Pannu, N. S.; Read, R. J.; Rice, L. M.; Simonson, T.; Warren, G. L. Crystallography & NMR system: A new software suite for macromolecular structure determination. *Acta. Crystallogr., Sect. D* **1998**, *54* (Pt 5), 905−21.
(26) McRee, D. E. XtalView/Xfit- -A versatile program for manipulating atomic coordinates and electron density. *J. Struct. Biol.* **1999**, *125* (2−3), 156−65.
(27) Kleywegt, G. J.; Jones, T. A. Software for handling macromolecular envelopes. *Acta Crystallogr., Sect. D* **1999**, *55* (Pt 4), 941−944.
(28) Laskowski, R. A.; MacArthur, M. W.; Moss, D. S.; Thornton, J. M. PROCHECK: a program to check the stereochemical quality of protein structures. *J. Appl. Crystallogr.* **1993**, *26* (Part 2), 283−291.
(29) Lovell, S. C.; Davis, I. W.; Arendall, W. B., III; de Bakker, P. I.; Word, J. M.; Prisant, M. G.; Richardson, J. S.; Richardson, D. C. Structure validation by Calpha geometry: phi, psi and Cbeta deviation. *Proteins* **2003**, *50* (3), 437−50.
(30) Pettersen, E. F.; Goddard, T. D.; Huang, C. C.; Couch, G. S.; Greenblatt, D. M.; Meng, E. C.; Ferrin, T. E. UCSF Chimera-A visualization system for exploratory research and analysis. *J. Comput. Chem.* **2004**, *25* (13), 1605−12.
(31) Merritt, E. A.; Bacon, D. J. Raster3D: Photorealistic Molecular Graphics. *Methods Enzymol.* **1997**, *277*, 505−524.
(32) Kirchhoff, W. EXAM: A two-state thermodynamic analysis program. In *National Institute of Standards and Technology Technical Note 1401*; National Institute of Standards and Technology, U.S. Department of Commerce Technology Administration: Washington, DC, 1993.
(33) Becktel, W. J.; Schellman, J. A. Protein stability curves. *Biopolymers* **1987**, *26* (11), 1859−77.
(34) Bonnet, R.; Dutour, C.; Sampaio, J. L.; Chanal, C.; Sirot, D.; Labia, R.; De Champs, C.; Sirot, J. Novel cefotaximase (CTX-M-16) with increased catalytic efficiency due to substitution Asp-240→Gly. *Antimicrob. Agents Chemother.* **2001**, *45* (8), 2269−75.
(35) Methods for dilution antimicrobial susceptibility tests for bacteria that grow aerobically, 4th ed. Approved standards M7-A4. In *National Committee for Clinical Laboratory Standards*; University of Villanova: Villanova, PA, 1997.

Table 1. Inhibition Constants against CTX-M-9 and CTX--16

Compounds		K_i (μM) for :	
		CTX-M-9 (Asp240)	CTX-M-16 (Gly240)
1	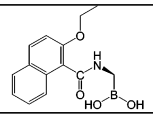	1.2	3.0
2	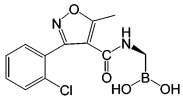	51	-
3	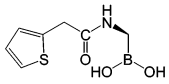	5.5	2.8
4	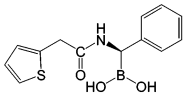	18.1	14
5	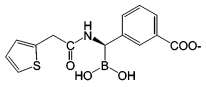	0.578	0.423
6	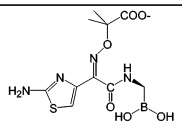	0.015	0.004
Cefoxitin	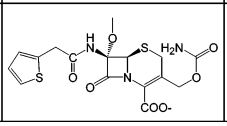	14.0[a]	-

[a] IC_{50}.

incubation compared to no incubation. Since **5** is about 100-fold weaker as an inhibitor than compound **6**, for which this incubation effect is at best slight, this effect cannot be attributed to simply tight binding, and seems to reflect something peculiar to this transition-state analogue. Compound **5** also shows time-dependent inhibition with the class C β-lactamase AmpC and the class A β-lactamase TEM-1. For all three enzymes, it forms a tetrahedral adduct mimicking a deacylation transition state, affecting the environment of or actually displacing the deacylation water. Whereas no significant structural reorganization is observed between any of these complexes and the corresponding apo-enzyme structures, it may be that binding of this transition-state analogue subtly tightens the enzyme, perhaps through the displacement of key waters, and that there is a kinetic barrier to these displacements.

The differential affinities of the glycylboronic acids allowed us to determine the contributions of the different functionalities on the R1 side chains, typical of β-lactams, to molecular recognition by CTX-M-9 and CTX-M-16. The K_i values ranged from 51 μM to 4 nM (Table 1). Surprisingly, the R1 side chain of ceftazidime (compound **6**), which is one of the worst substrates of CTX-M enzymes, conferred a K_i value 350-fold higher than that conferred by the cephalothin R1 side chain, the best substrate of CTX-M enzymes.[4] CTX-M-16, which is more active against ceftazidime than CTX-M-9, is also 4-fold more susceptible than CTX-M-9 to this ceftazidime analogue inhibitor.

Adding an *m*-carboxyphenyl group to the cephalothin-like glycylboronic acid (compound **5**), which is meant to imitate the completely conserved C(3)4′ carboxylate of β-lactams, improved CTX-M inhibition by 10-fold (compared to compound **3**, Table 1). However, addition of the phenyl ring of compound **4** increased the K_i value by 3-fold with respect to compound **3**, a trend opposite to that observed with the class C β-lactamase AmpC and with the class A enzyme TEM-1.[19] Comparing compound **4** to **5** suggests that the carboxylate alone adds about 2 kcal/mol to affinity, broadly consistent with the importance of this group to recognition by such β-lactamases.

X-ray Crystallographic Structure Determination. To investigate the structural bases for the relative affinities and to understand the details of recognition along the reaction coordinate, we determined the crystal structures of CTX-M enzymes in complex with compounds **1**, **5**, **6**, and cefoxitin to resolutions between 1.16 and 1.70 Å (Table 2). Excluding proline and glycine, 98.1 to 98.3% of residues were in the favored region and 1.7 to 1.9% of residues were in the allowed region of the Ramachandran plot.[29] The root-mean-square deviation (RMSD) of the Cα positions is approximately 0.31 Å between the two monomers of crystallographic asymmetric unit, and each monomer varies from 0.17 to 0.24 Å from complex to complex, showing no dramatic change of the overall active site geometry.

At the ultrahigh resolution of the structure with compound **5** (1.16 Å), it became clear that the molecules in the crystal consisted of both the apo and complex states at approximately a 1:1 ratio. The electron densities of the apo state water molecules and the phosphate molecule replaced by the ligand were clearly visible in the active site, overlapping the density for the compound. Interestingly, no double conformations were revealed for the active site residues except for Lys73, suggesting that the active site configuration of the apo-enzyme broadly resembles that of the deacylation transition-state complex.

Hydrolytic Pathway: The Transition States. In all structures, the position of inhibitors in the active site was unambiguously identified in the initial $F_o - F_c$ electron density difference map contoured at 3σ (Figure 3). Electron density connects the Oγ of the catalytic Ser70 to the boron atom of the glycylboronic acids and to the C8 atom of cefoxitin. The geometry of the boronic acid group was tetrahedral (Figures 4 and 5), whereas the ester group of the cefoxitin adduct was planar, as expected (Figure 4A and 4B).

Cefoxitin formed typical interactions with the active site residues. Its O9 carbonyl made hydrogen bonds with the N backbone atoms of residues 70 and 237, which form the "oxyanion" hole of class A enzymes.[36] In the glycylboronic acid complex structures, the O9a boronic acid hydroxyl adopted the same conformation and also hydrogen bonded with the "oxyanion" hole nitrogen and the O backbone atom of residue 237 (Figures 4B and 5).

The boronic acid hydroxyl O9b of compounds **1** and **6** interacted with Oγ of Ser130 and a well-ordered water molecule W2 (Figure 5A and 5C). This O9b atom represents the lactam nitrogen leaving group of the substrate in the acylation transition state, and it is comforting to see that its position corresponds closely to that of the N5 atom of the six-member ring in the cefoxitin complex. For compound **5**, the O9b of the boronic

(36) Murphy, B. P.; Pratt, R. F. Evidence for an oxyanion hole in serine beta-lactamases and DD-peptidases. *Biochem. J.* **1988**, *256* (2), 669−72.

Table 2. X-ray Crystallographic Statistics

complex (compound/enzyme)	**1**/CTX-M-9	**5**/CTX-M-9	**6**/CTXM-9	**6**/CTX-M-14	cefoxitin/CTX-M-9
cell constants (Å; deg)	$a = 45.26$ $b = 106.8$ $c = 47.87$ $\beta = 101.74$	$a = 45.11$ $b = 106.67$ $c = 47.71$ $\beta = 101.88$	$a = 45.18$ $b = 106.84$ $c = 47.88$ $\beta = 101.90$	$a = 45.31$ $b = 106.89$ $c = 44.88$ $\beta = 101.87$	$a = 45.21$ $b = 106.78$ $c = 47.78$ $\beta = 101.62$
resolution (Å)	1.60 (1.66−1.60)[a]	1.12 (1.16−1.12)	1.25 (1.29−1.25)	1.35 (1.40−1.35)	1.70 (1.76−1.70)
total reflections	302 202	1 294 296	592 381	354 328	261 682
unique reflections	57 897	143 714	113 498	76 672	48 520
R_{merge} (%)	6.9 (34.7)	5.4 (28.7)	3.4 (25.9)	2.9 (11.4)	6.2 (34.1)
completeness (%)	98.6 (96.7)	85.1 (23.1)[b]	92.7 (76.9)	78.6 (26.6)[b]	99.8 (99.8)
[I]/[σ(I)]	11.0 (2.5)	22.9 (1.9)	15.9 (2.1)	15.2 (3.3)	13.2 (3.0)
resolution range for refinement (Å)	20−1.6	20−1.12	20−1.25	20−1.35	20−1.70
number of protein residues	524	523	523	523	523
number of water molecules	804	861	868	864	647
RMSD bond length (Å)	0.009	0.006	0.005	0.004	0.009
RMSD angle[c] (deg)/ angle distance[d] (Å)	1.53[c]	0.022[d]	0.020[d]	0.016[d]	1.55[c]
R-factor (%)	15.7	10.7	12.9	12.9	15.8
R_{free}[e] (%)	19.3	14.0	16.8	17.1	19.7

[a] Values in parentheses are for the highest resolution shell used in refinement. [b] Values in parentheses are for the highest resolution shell information used in refinement. For the **5**/CTX-M-9 complex, the highest resolution shell with completeness of 50% or better was 1.21 to 1.16 Å (50% complete), whereas for the **6**/CTX-M-14 complex, the same shell was 1.52 to 1.45 Å (62.3% complete) [c] Refined by CNS1.1. [d] Refined by SHELXL-97. [e] R_{free} was calculated with 5% of reflections set aside randomly.

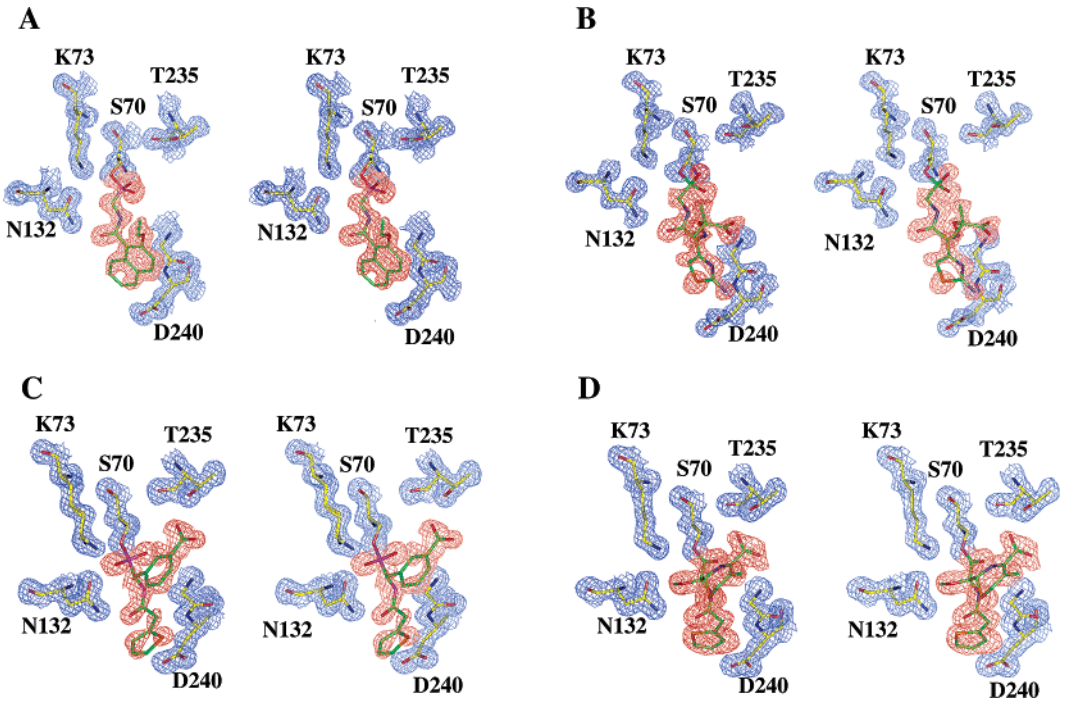

Figure 3. Stereoviews of the active site electron density for each complex structure. For each, the $2F_o - F_c$ electronic density of the refined model of CTX-M-9 is shown in blue, contoured at 1σ, and the simulated-annealing omit electron density of the ligand is shown at 3σ in red for compound **1** (A), compound **6** (B), compound **5** (C), and cefoxitin (D). Carbon atoms are yellow for the protein or green for the adduct; oxygen atoms are red, and nitrogen atoms are blue.

acid flipped by 109° and interacted with the residues Asn170 and Glu166, replacing the catalytic water molecule, which is not present in this structure (Figures 4 and 5B). In this structure, the O9b atom represents the position of the catalytic water in the deacylation transition state, consistent with similar interactions observed in a TEM-1 boronic acid structure.[37]

Overall, the boronic acid complexes of compounds **1** and **6**, which display only the R1 side chain of β-lactams (Figure 1), adopted a conformation in the active site consistent with acylation transition-state analogues; compound **5** adopted a conformation consistent with a deacylation transition-state analogue.[38] The cefoxitin complex represented the acyl-enzyme intermediate between these two high-energy intermediates.

Interactions between CTX-M and 7α-Substituted β-Lactam. The X-ray crystal structure of cefoxitin bound to CTX-M-9 provided insights into the interactions of the 7α-substituted

(37) Ness, S.; Martin, R.; Kindler, A. M.; Paetzel, M.; Gold, M.; Jensen, S. E.; Jones, J. B.; Strynadka, N. C. Structure-based design guides the improved efficacy of deacylation transition state analogue inhibitors of TEM-1 beta-Lactamase. *Biochemistry* **2000**, *39* (18), 5312−21.

(38) Strynadka, N. C.; Martin, R.; Jensen, S. E.; Gold, M.; Jones, J. B. Structure-based design of a potent transition state analogue for TEM-1 beta-lactamase. *Nat. Struct. Biol.* **1996**, *3* (8), 688−95.

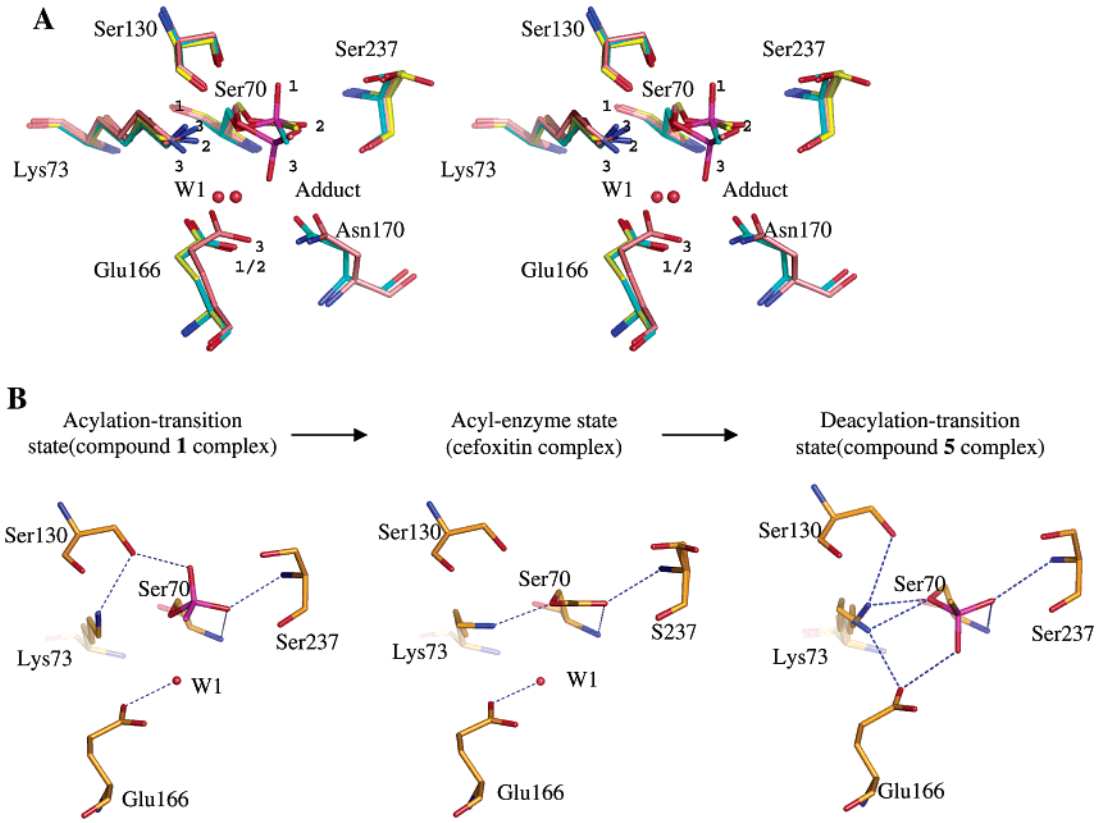

Figure 4. Movements of residues Lys73 and Glu166 in the CTX-M-9-complex structures with compounds **1**, **5**, and cefoxitin. (A) Stereoview of superimposed complexes with compound **1** (acyl-transition state, cyan, step 1), cefoxitin (acyl-enzyme, yellow, step 2), and compound **5** (deacylation-transition state, pink, step 3) showing the progression of the hydrolytic reaction. Different configurations of Lys73, Glu166, and the covalent adduct are indicated by the three step numbers. (B) Key polar interactions observed between the adducts and residues Ser70, Lys73, Ser130, Glu166, and Ser237 during the progression of the hydrolytic reaction. Only the boronic acid group and the carbonyl ester are shown for glycylboronic acids and cefoxitin, respectively.

β-lactams with class A enzymes. Overall, the cefoxitin complex was consistent with the acyl-enzyme complexes previously observed in Toho-1 enzyme.[9] A key difference was that the bulky 7α-methoxy substituent of cefoxitin, which in the substrates is a hydrogen, was 3.0 Å from the Oδ1 atom of Asn132, suggesting an electrostatic and steric clash. This clash is consistent with the destabilization of the enzyme by the formation of the cefoxitin acyl-enzyme adduct (below) and with structural observations in other complexes between 7α-containing inhibitors and β-lactamases.[14,39] Despite this clash, no rearrangement of the residues surrounding the compound is observed. Most critically, the catalytic water is present in this structure, though it is displaced (by 1 Å) relative to the complex structures with acyl-transition-state analogues (Figure 4A). This observation is interesting because cefoxitin, along with similar inhibitors such as moxalactam and imipenem, has been proposed to inhibit β-lactamases by displacing the catalytic water from the active site. Instead, these inhibitors may act by blocking the formation of the deacylation transition state. When the cefoxitin complex is superimposed on that of the deacylation transition state analogue, the C7b of the cefoxitin 7α-methoxy group is placed 1.4 Å away from the O9b hydroxyl atom of the transition-state analogue (compound **5**). This oxygen represents the position of the deacylating water in the deacylation transition state; the placement of the 7α-methoxy group seems thus to block the formation of the transition state.

Other Interactions. The dihydrothiazine ring of cefoxitin and the carboxy-phenyl ring of **5** represent the five- and six-membered rings typical of penicillins and cephalosporins, in the acyl-enzyme and deacylation high-energy intermediate forms, respectively. The ring S1/C1 and C2 atoms of cefoxitin and compound **5** make van der Waals contacts with the aromatic ring of Tyr105 (distances ranging from 3.5 to 4.7 and 3.3 to 4.6 Å, respectively; see Table 3 for numbering). For compound **5**, the ring C5 atom is 3.0 Å from the Ser130 Oγ atom, with the hydroxyl group perpendicular to the face of the ring, suggesting a dipole−quadrupole interaction. The carboxylic acid groups of compound **5** and cefoxitin interact with Oγ1 of Thr235 and three well-ordered water molecules, consistent with the inhibitor carboxylate mimicking the ubiquitous C(3)4′ substrate carboxylate, as previously observed in TEM complexes.[40] Surprisingly, Arg-276, which is implicated in the catalytic process of CTX-M enzymes,[11,41] is disordered, and multiple conformations are modeled. In one monomer, both conformations interact with the *m*-carboxy six-member ring side chain of compound **5** via an ordered water molecule (Figure 5B). Another atypical feature is the absence of interaction with Oγ of residue Ser237, which had been previously observed in the acyl-enzyme complexes of Toho-1.[9]

(39) Wang, X.; Minasov, G.; Shoichet, B. K. Noncovalent interaction energies in covalent complexes: TEM-1 beta-lactamase and beta-lactams. *Proteins* **2002**, *47* (1), 86−96.

(40) Wang, X.; Minasov, G.; Blazquez, J.; Caselli, E.; Prati, F.; Shoichet, B. K. Recognition and resistance in TEM beta-lactamase. *Biochemistry* **2003**, *42* (28), 8434−44.

(41) Gazouli, M.; Legakis, N. J.; Tzouvelekis, L. S. Effect of substitution of Asn for Arg-276 in the cefotaxime-hydrolyzing class A beta-lactamase CTX-M-4. *FEMS Microbiol. Lett.* **1998**, *169* (2), 289−93.

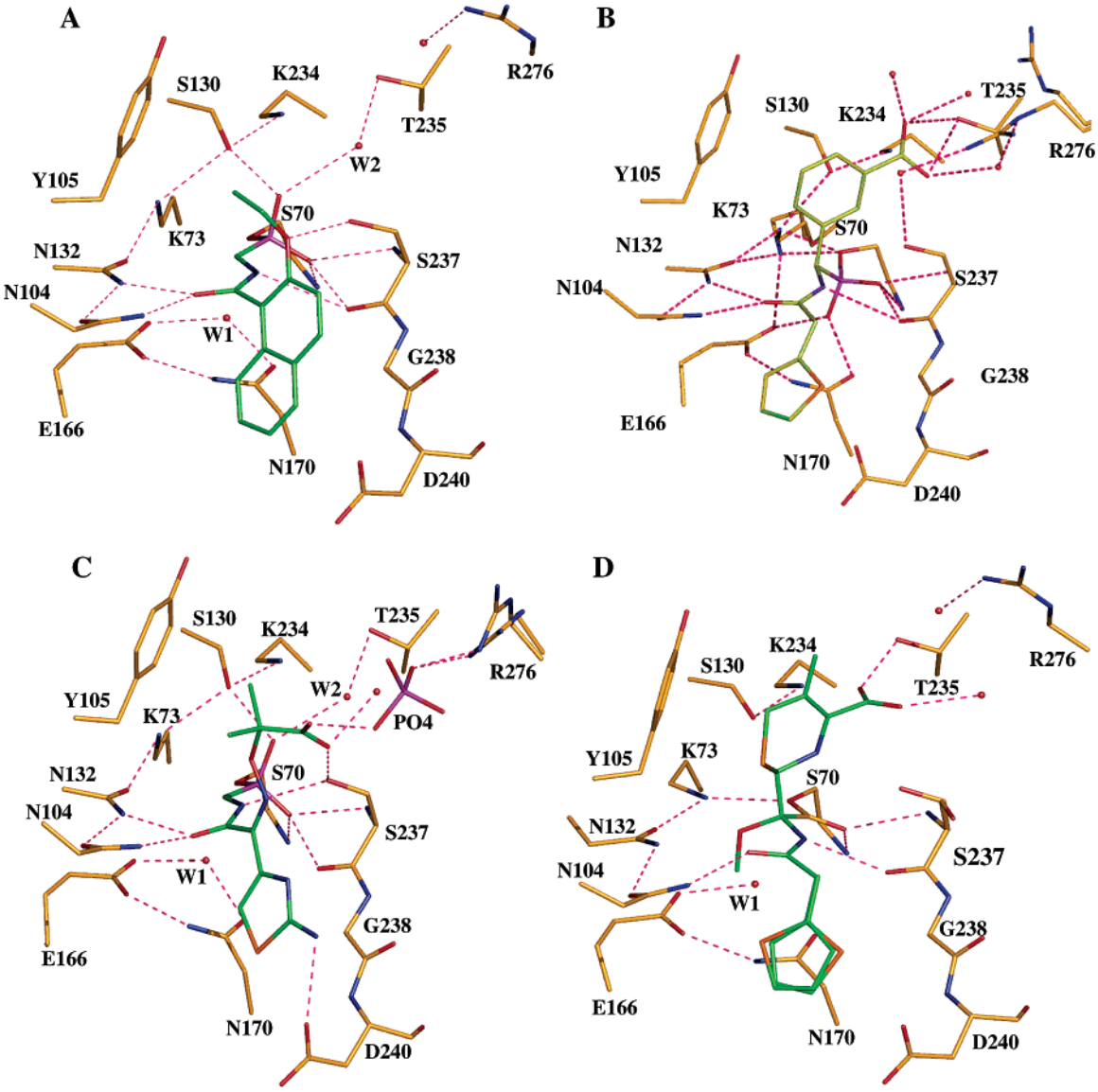

Figure 5. Key polar interactions observed between CTX-M-9 and compounds **1** (A), **5** (B), **6** (C), and cefoxitin (D). Carbon atoms are yellow for the protein or green for the adduct; oxygen atoms, red; nitrogen atoms, blue; phosphate atoms, violet.

The R1 side chain amide groups of all inhibitors are placed close to where the analogous R1 side chain amide is in the complexes between β-lactams and class A β-lactamases.[42] The O12 amide oxygen of this side chain hydrogen bonds with the Nδ2 atom of Asn132, except perhaps in the cefoxitin complex where this distance rises to 3.4 Å because of the clash between the 7α-methoxy substituent of cefoxitin and the same Nδ2 atom (Figure 5D). As previously observed in the Toho-1 acyl-enzyme complexes,[9] an interaction of this amide oxygen (O12) is observed with the Nδ2 atom of Asn104, which is not present in TEM enzymes, but is conserved in CTX-M enzymes. The N atom (N10) of the R1 amide side chain hydrogen bonds with the backbone O atom of residue 237 for the glycylboronic acids **1**, **5**, and cefoxitin (distances 2.9 to 3.0 Å), which is a widely observed interaction. For compound **6** (the ceftazidime-like compound), the distance between the N10 and O backbone atom of residue 237 is less favorable: 3.3−3.4 Å in the complexes with CTX-M-9 and CTX-M-14. Instead, the Oγ atom of Ser237 appears to hydrogen bond with this ligand atom, at least in the complex with CTX-M-9 (Figure 5C).

The nanomolar inhibition of compound **6** may be due to additional interactions of its carboxypropyl-oxyimino group with Asn104, Ser237, and Arg276 (Figure 5C). The oxyimino atom (O13b) hydrogen bonds with the Oγ atom of Ser237. This interaction is conserved in another potent inhibitor, compound **1**, which has an equivalent oxygen linker atom (O13b). The carboxylate of compound **6** forms a charged dipole hydrogen bond with the Oγ atom of Ser237, whereas its neighboring propyl group makes van der Waals interactions with the phenyl ring of Tyr105 (distances 3.6−4.6 Å). In some monomers, the carboxylate group of compound **6** interacts with one conformation of Arg276 (Figure 5C) and Ser274 via a bound phosphate molecule.

Movements of Catalytic Residues Lys73 and Glu166. The conformations of the catalytic residues Lys73 and Glu166 appear to change according to the progression along the reaction coordinate. Since both residues have been mooted as possible

(42) Strynadka, N. C.; Adachi, H.; Jensen, S. E.; Johns, K.; Sielecki, A.; Betzel, C.; Sutoh, K.; James, M. N. Molecular structure of the acyl-enzyme intermediate in beta-lactam hydrolysis at 1.7 Å resolution. *Nature* **1992**, *359* (6397), 700−5.

Table 3. Key Interactions in the Complex Structures

Complexes	**1**/CTX-M-9	**5**/CTX-M-9	**6**/CTXM-9	**6**/CTXM-14	**Cefoxitin**/CTX-M-9
Numbering of compound atoms	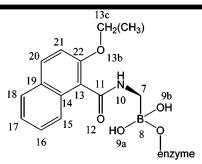	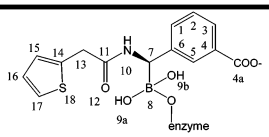	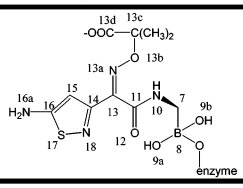		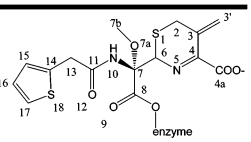
Distance between key residues of the binding site[a] **:**					
Catalytic water – S70 Oγ	2.75 ; 2.72	N.P.	2.71 ; 2.69	2.73 ; 2.75	3.41 ; 3.41
Catalytic water – E166 Oε1	2.50 ; 2.48	N.P.	2.56 ; 2.53	2.59 ; 2.51	2.46 ; 2.46
Catalytic water – N170 Oδ1	2.64 ; 2.74	N.P.	2.72 ; 2.73	2.75 ; 2.71	3.27 ; 3.32
K73 Nζ – S70 Oγ	3.09 ; 3.01	2.83/2.56[b] ; 2.84/2.61	3.21 ; 3.08	3.15 ; 3.09	2.64 ; 2.77
K73 Nζ – E166 Oε1	4.05 ; 3.95	2.82/3.60 ; 2.76/3.50	4.21 ; 4.14	4.18 ; 4.16	3.25 ; 3.43
K73 Nζ – N132 Oδ1	2.75 ; 2.68	2.92 /2.55 ; 3.00/2.56	2.72 ; 2.69	2.74 ; 2.78	2.92 ; 2.78
K73 Nζ – S130 Oγ	2.94 ; 2.94	4.06/3.07 ; 4.07/3.10	2.93 ; 2.86	2.93 ; 2.89	3.26 ; 3.22
K234 Nζ – S130 Oγ	2.87 ; 2.91	2.85 ; 2.86	2.84 ; 2.87	2.82 ; 2.85	2.80 ; 2.70
Distance between key residues of the binding site and compound atoms					
S70N - O9a / O9	2.86 ; 2.85	2.83 ; 2.83	2.84 ; 2.79	2.81 ; 2.81	2.86 ; 2.91
S237N - O9a / O9	2.78 ; 2.76	3.00; 2.95	2.75 ; 2.77	2.81 ; 2.78	2.78 ; 2.76
S237O - O9a	2.76 ; 2.71	2.73 ; 2.68	2.75 ; 2.73	2.72 ; 2.75	2.79 ; 2.72
S130Oγ - O9b / C5 / N5	2.63 ; 2.69	3.11 ; 3.14	2.71 ; 2.70	2.72 ; 2.73	3.39 ; 3.37
E166Oε1 - O9b	N.P.	2.78 ; 2.68	N.P.	N.P.	N.P.
N170Oδ1 - O9b	N.P.	2.54 ; 2.58	N.P.	N.P.	N.P.
T235Oγ1 - COO^-4a	N.P.	2.48 ; 2.48	N.P.	N.P.	2.41 ; 2.39
K234Nζ - COO^-4a	N.P.	3.57 ; 3.48	N.P.	N.P.	3.47 ; 3.55
S237O - NH10	3.12 ; 3.15	3.13 ; 3.10	3.39 ; 3.36	3.35 ; 3.41	2.86 ; 2.99
S237Oγ - NH10	3.46 ; 3.55/5.06	3.92 ; 3.73	3.15 ; 3.13	3.23 ; 3.37	3.58 ; 3.62/5.15
S237Oγ - O13b	2.75 ; 2.70/3.48	N.P.	3.49 ; 3.33	3.32 ; 3.32	N.P.
S237Oγ - COO^-13d	N.P.	N.P.	2.83 ; 2.73	2.84 ; 2.82	N.P.
N132Nδ2 - O12	2.64 ; 2.69	2.71 ; 2.77	2.84 ; 2.77	2.83 ; 2.82	3.38 ; 3.27
N104Nδ2 - O12	2.88 ; 2.86	2.97 ; 2.93	2.98 ; 2.95	2.95 ; 2.96	3.04 ; 2.97
D240Oδ1 - N16a/CH18	3.17 ; 3.15	N.P.	2.83 ; 2.84	2.81 ; 2.84	N.P.

[a] Two distances in monomer A and B are shown. [b] In cases with two distances shown within one monomer, multiple conformations are present.

catalytic bases for the reaction, this movement seems noteworthy. In moving from the apo-enzyme to the acylation transition state complex with compound **1**, Lys73 side chain switches from two conformations in the apo state[13] to only one in the transition state analogue structure in which the Nζ atom of Lys73 hydrogen bonds with the Oγ atom of residue Ser130 (Figure 4). In the cefoxitin acyl-enzyme complex, the following step of the catalytic pathway, the Nζ atom of Lys73 rotates by 50° to hydrogen-bond with the Oγ atom of the hydrolytic Ser70 and the Oδ1 atom of Asn132 (Figure 4B). In the deacylation transition state, double conformations in the two monomers were observed. Conformation 1 hydrogen-bonds with both the Oγ atom of Ser70 and the Oϵ2 atom of Glu166, which is implicated in the activation of the catalytic water molecule during the deacylation process in class A β-lactamases (Figure 5B). Conformation 2 hydrogen-bonds with Ser70 and Ser130. Although the structure with compound **5** is a mixture of the apo and complex forms, two conformations of Lys73 appear to exist in both states. This is based on comparing the occupancies of the two conformations in this 1.16 Å structure and those in previously determined ultrahigh-resolution apo structures.[13] Corresponding to the conformational changes of Lys73 along the reaction coordinate, the side chain of Glu166 also changes conformation. From the apo-enzyme to acylation transition state and acyl-enzyme intermediate, Glu166, together with the catalytic water, moves by 0.4 to 0.6 Å away from the ligand. In the deacylation transition state, the Glu166 side chain shifts back toward the ligand and assumes a conformation similar to that in the apo-enzyme.

Thermal Denaturation Experiments. To analyze the noncovalent interaction energy of cefoxitin with CTX-M-9, the enzyme was thermally denatured alone and in complex with cefoxitin. For the apo-enzyme, an average T_m value of 47.9 °C and an average van't Hoff enthalpy (ΔH_{VH}) value of 142 kcal/mol were obtained at a ramp rate of 2 °C/min. On rapid cooling, 100% of the original fluorescence signal returned. When unfolded enzyme was slowly cooled at 2 °C/min back through the folding transition, an average T_m of 47.6 °C and an average ΔH_{VH} value of 134 kcal/mol were obtained. Similar results were obtained with cefoxitin complex: more than 98% of the original signal returned after rapid cooling, and T_m and ΔH_{VH} values were similar during the unfolding and folding steps (the T_m was 39.5 °C, whereas the temperature of refolding was 38.8 °C, with the corresponding ΔH_{VH} being 122 and 79 kcal/mol, respectively). These results suggested that the apo-enzyme and the corresponding complex with cefoxitin were reversibly denatured by temperature in a two-state manner. Compared to the apo form of CTX-M-9, the cefoxitin complex was destabilized by 8 °C (Figure 6), equivalent to a decrease in stability of −3.7 kcal/mol. This suggests that cefoxitin actually makes unfavorable noncovalent interactions with the enzyme within the covalent complex.

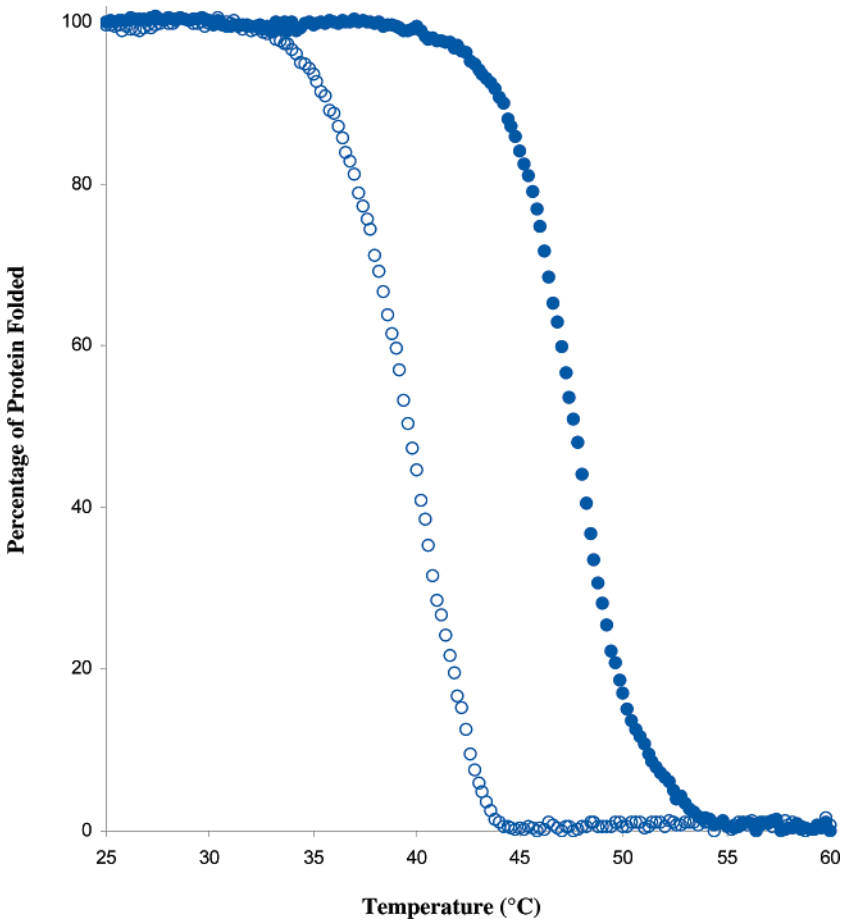

Figure 6. Reversible, two-state thermal denaturation of CTX-M-9 alone and with cefoxitin as monitored by fluorescence signal. Solid circles indicate CTX-M-9 enzyme, and open circles indicate CTX-M-9 in its covalent adduct with cefoxitin.

Table 4. Inhibitor MICs

	MICs (μg/mL) for *E. coli* producing:	
	CTX-M-9 (Asp240)	CTX-M-16 (Gly240)
cefotaxime	128	128
cefotaxime and compound **1**	64	64
cefotaxime and compound **2**	128	128
cefotaxime and compound **3**	32	32
cefotaxime and compound **4**	128	128
cefotaxime and compound **5**	16	16
cefotaxime and compound **6**	4	4

Microbiology. The inhibition activities of the glycylboronic acids were investigated against clinical CTX-M-producing *E. coli*. When cefotaxime and glycylboronic acids were administrated alone in a disk diffusion assay, they had little activity on bacteria growth, as expected. However, compounds **1**, **3**, **5**, and **6** in combination with cefotaxime produced a large inhibition halo surrounding the disk (data not shown). This inhibition of the bacterial growth revealed clear synergy between these compounds, with the size of the inhibition zone inversely correlated with K_i values. For compounds **2** and **4**, no synergy was observed.

After the synergy test, antimicrobial activity was investigated quantitatively to determine the minimum inhibitory concentrations (MICs) of the cefotaxime/inhibitor combination necessary to inhibit the bacterial growth (Table 4). The MICs of cefotaxime alone against the CTX-M-producing *E. coli* strains were 128 μg/mL, which corresponds to a high level of resistance according to the NCCLS standards.[35] No glycylboronic acids had measurable antibiotic activity when used alone. In combination with cefotaxime, compounds **3**, **5**, and **6** decreased MIC values significantly, from 128 μg/mg to 32, 16, and 4 μg/mL, respectively. The other compounds had no significant effect. As observed with the disk diffusion method, the MICs were monotonically correlated with the K_i values.

Discussion

Our interest here was to capture snapshots of the CTX-M β-lactamases along their reaction coordinate, with a view to understand their activities and to provide templates for inhibitor discovery. Three key observations emerge from this study. First, Glu166 and Lys73, which have been proposed as catalytic bases, move in coordination with progression along the reaction coordinate. Second, these structures suggest a mechanism of inhibition for the 7α-substituted β-lactams that may be general to class A and class C β-lactamases, despite their very different mechanisms. Third, several of the reagents used to probe the mechanism of the CTX-Ms turn out to be potent inhibitors and may be lead to drug discovery efforts against these enzymes.

Reaction Coordinate. β-Lactam hydrolysis by serine β-lactamases may be thought of as having three low-energy and two high-energy intermediates. The low-energy intermediates are the precovalent complex, the Ser70-bound covalent intermediate, and the postcovalent product complex. Between these states are the acylation and deacylation tetrahedral intermediates; each of these is flanked by two transition states: one early stage

transition state, involving the attack of a nucleophile on a planar carbonyl, and one late stage transition state, involving collapse of the tetrahedral center as a leaving group departs (four transition states in total).[43] In acylation, the nucleophile for the first transition state is the Ser70Oγ, and the leaving group for the second transition state is the lactam nitrogen. For deacylation, the nucleophile for the first transition state is the hydrolytic water and the leaving group for the second transition state is the Ser70Oγ. Before considering the movements of Glu166 and Lys73 as the reaction proceeds, it is useful to consider which transition states are being mimicked by the complexes determined here.

The transition states may be distinguished by the groups that are activated for attack and departure. In the complex with compound **6**, the distance between Ser130Oγ and the second boronic oxygen is 2.7 Å; this resembles the second acylation transition state since Ser130 is thought to be the catalytic acid that activates the lactam leaving group, which the boronic oxygen represents. Also, this distance is shorter than that between Lys73 Nζ and Ser70Oγ (3.2 Å), an interaction thought to activate Ser70 for the initial hydrolytic attack. The Lys73 Nζ has moved closer to Ser130Oγ (3.0 Å) than Ser70Oγ, whereas the opposite is true in the apo CTX-M structures where the Nζ interacts more closely with Ser70Oγ.

The complex with compound **5** may also correspond to a late stage transition state, this time of the deacylation step. In one of the two conformations of Lys73 observed in this structure, the hydrogen bond between Lys73Nζ and Ser70Oγ has tightened to 2.5 Å, closer than the 2.7 Å observed in the acyl-enzyme complex; this interaction may reflect the activation of the Ser70Oγ for leaving the tetrahedral center, releasing product. Correspondingly, the distance between Glu166Oϵ1 and the boronic group oxygen that mimics the deacylating water has lengthened to 2.8 Å, an increase from the 2.6 Å distances typically observed in the apo, acylation, transition-state, and acyl-enzyme structures. Thus, the complexes with both compounds **6** and **5** may represent second stage, breakdown transition-states, the former for acylation and the latter for deacylation of the enzyme by a β-lactam substrate.

Together with previous studies of the apo-enzyme,[10,13] these structures thus give us views of four steps along the reaction coordinate. Perhaps the most compelling observation to emerge from considering these together is the coordinated movement of substrate and enzyme groups as the reaction progresses. In these structures, the substrate analogues invert configuration between the tetrahedral acylation transition state and the planar acyl-intermediate and between the planar intermediate and the deacylation transition state. More interestingly still, the conformations of the key catalytic residues Glu166 and Lys73 change from structure to structure along the reaction coordinate.

The Lys73 side chain, which is essentially unmoving in TEM and SHV complexes, changes conformation in CTX-M enzymes in a manner apparently coordinated with progression along the reaction coordinate (Figure 4). In the apo-enzymes Toho-1 and CTX-M-9, double conformations were observed for this residue. Conformation 1 of Lys73 is oriented toward Ser70,[10] suggesting that in CTX-M enzymes Lys73 might help to activate this catalytic residue for attack on the β-lactam ring. Conformation 2 moves closer to Ser130, which has been implicated as the catalytic acid for activating the lactam nitrogen leaving group on the substrate. In the acyl-transition state structures, the Lys73 side chain adopts only one conformation, closely resembling conformation 2 in the apo state, hydrogen bonding with the Oγ atom of Ser130 (Figure 4B). Subsequently, in the acyl-enzyme, the Lys73 side chain switches to a single conformation closer to conformation 1 of the apo-enzyme, with its Nζ atom at equal hydrogen-bonding distances with the Oγ atom of Ser70 (Figure 4B) and Oδ2 atom of Asn132. These interactions may increase the polarization of the ester bond to Ser70, increasing the reactivity of the acyl-enzyme intermediate. In the deacylation transition-state structure, the Lys-73 side chain again has the two conformations observed in the apo-enzyme (Figure 4B). The close contact that Lys73 maintains with Ser70 in both conformations suggests that the lysine may help stabilize the negative charge buildup in the deacylation transition state.

Like Lys73, Glu166 also changes conformations along the reaction coordinate, albeit less dramatically (Figure 4). In the acyl-transition-state and the acyl-enzyme structures, the side chain of Glu166 and the catalytic water molecule move by about 0.5 Å away from the ligand relative to the apo-enzyme structure. In the deacylation-transition-state structure the Glu166 side chain shifts back toward the adduct (Figure 4A). When we superimpose the acyl-transition-state structure of TEM-1 (PDB1M40) with its apo-enzyme (PDB 1JWP),[7,44] the same movement is observed, though this was not previously reported. These movements may reflect the presence of the ligand in the active site, which displaces the catalytic water molecule due to a steric clash between it and the C7 atom of the ligand. In the deacylation-transition-state structure, where the C7 atom is displaced owing to the inversion of the tetrahedral center, this potential clash is relieved and Glu166 relaxes back toward the ligand.

Acyl-Enzyme Complex. Acyl-enzyme complexes have been previously determined for Toho-1, a member of the broad CTX-M family. In the structures, the substitution of Glu166Ala created a deacylation deficient enzyme, allowing substrate complexes to be captured in their acyl-enzyme adducts.[9] Here, an acylation complex was obtained with wild-type CTX-M-9 using the β-lactam antibiotic cefoxitin (Figure 4D). Cefoxitin is a member of a class of β-lactams including imipenem and moxalactum that replace a hydrogen on the α-face of the β-lactam ring with a bulkier group, converting substrates into inhibitors. These bulky groups have been proposed to displace the deacylation water in class A β-lactamases, leading to inhibition. Our structure is inconsistent with this hypothesis: whereas the hydrolytic water is displaced by 1 Å, it is nevertheless clearly present in the active site and is still interacting with the same catalytic residues as it does in other class A β-lactamase structures.

Our structure also differs from a cefoxitin complex structure previously obtained with the class A β-lactamase of *Bacillus licheniformis* BS3.[45] In this complex, cefoxitin is in an unusual position and induces a major rearrangement of the binding site. In our complex structure, conversely, cefoxitin assumes a

(43) Lobkovsky, E.; Billings, E. M.; Moews, P. C.; Rahil, J.; Pratt, R. F.; Knox, J. R. Crystallographic structure of a phosphonate derivative of the *Enterobacter cloacae* P99 cephalosporinase: mechanistic interpretation of a beta-lactamase transition-state analogue. *Biochemistry* **1994**, *33* (22), 6762−72.

(44) Minasov, G.; Wang, X.; Shoichet, B. K. An ultrahigh-resolution structure of TEM-1 beta-lactamase suggests a role for Glu166 as the general base in acylation. *J. Am. Chem. Soc.* **2002**, *124* (19), 5333−40.

configuration similar to that observed in acyl-intermediate complexes of Toho-1 E166A mutant. The backbone conformation of the Omega loop in the cefoxitin CTX-M-9 complex more closely resembles that adopted in the apo structures of TEM-1,[7] CTX-M-9,[13] and Toho-1[10] than that adopted in the acyl-enzyme structures obtained with the E166A mutant Toho-1. These data support the suggestion of Ibuka et al. that the conformation of the Omega loop observed in these last complexes is the consequence of the Glu166Ala substitution.[9,10] Thus, the structure reported here may be a better model of the conformation adopted by the native enzymes in their substrate acyl-enzyme intermediates.

How then does cefoxitin inhibit the CTX-M enzymes? The key of course is the unusual 7α substituent on the β-lactam ring. The superposition of the deacylation transition-state complex with the cefoxitin complex revealed that this 7α substituent is only 1.4 Å away from where the transition state would form during deacylation, as modeled by the complex with compound **5**. This would prevent the formation of this transition state and therefore block the progress of the reaction further than the acyl-intermediate. Both the destabilization of the enzyme in the cefoxitin complex and blocking the formation of the deacylation transition state are similar to what has been observed with the 7α-substituted β-lactams and other classes of β-lactamase, including TEM-1[39] and the class C β-lactamase AmpC.[14] Despite the very different reaction mechanisms of the class A and C enzymes and the large differences among 7(6)α-substituted inhibitors (e.g., cefoxitin, imipenem, moxalactam), all may share a common mechanism of inhibition (though other mechanisms are possible; see for instance ref 46).

Inhibition. Unexpectedly, several of the glycylboronic acids used here as reagents to study the reaction coordinate have turned out to be potent inhibitors of the CTX-M enzymes. These compounds span 3 orders of magnitude in affinity for CTX-M-9, from K_i values of 51 uM to 20 nM (Table 1). Most encouragingly, compound **6**, a ceftazidime-like boronic acid, inhibits CTX-M-16 with a K_i of 4 nM. The high potency of this compound as an enzyme inhibitor was reflected in its ability to reverse the bacterial resistance against cefotaxime in cell culture, decreasing the MIC of this third-generation cephalosporin by 32-fold. Intriguingly, compound **6** is also relatively potent versus the class C β-lactamase AmpC (K_i, 20 nM).[47] Compounds with good activity across classes of β-lactamases are very rare. The nanomolar activity of **6** against enzymes from both classes, coupled with its activity in cell culture, suggests that this inhibitor may be a good lead for generalist inhibitors to reverse bacterial resistance to clinically important β-lactamases.

Acknowledgment. Supported by NIH Grant GM63813 (to B.K.S.). R.B. was supported by L'Association pour l'Organization des Réunions Interdisciplinaires de Chimiothérapie Anti-Infectieuse (AORIC), Program Hospitalier de Recherche Clinique (PHRC) du Centre Hospitalier Universitaire de Clermont-Ferrand, and Ministère Français de l'Education Nationale de la Recherche et de la Technologie, and participated in this study as a sabbatical scholar at UCSF. We thank Ruth Brenk and Veena Thomas for reading the manuscript. We also thank Rolande Perroux, Marie-Héléne Desforges, Claudine Morge, Marléne Jan, and Dominique Rubio for assistance with bacterial strains.

JA042850A

(45) Fonze, E.; Vanhove, M.; Dive, G.; Sauvage, E.; Frere, J. M.; Charlier, P. Crystal structures of the *Bacillus licheniformis* BS3 class A beta-lactamase and of the acyl-enzyme adduct formed with cefoxitin. *Biochemistry* **2002**, *41* (6), 1877−85.

(46) Maveyraud, L.; Massova, I.; Birck, C.; Miyashita, K.; Samama, J. P.; Mobashery, S. Crystal Structure of 6alpha-hydroxymethylpenicillinate complexed to the TEM-1 beta-lactamase from *Escherichia coli*: evidence on the mechanism of action of a novel inhibitor designed by a computer-aided process. *J. Am. Chem. Soc.* **1996**, *118*, 7435.

(47) Powers, R. A.; Caselli, E.; Focia, P. J.; Prati, F.; Shoichet, B. K. Structures of ceftazidime and its transition-state analogue in complex with AmpC beta-lactamase: implications for resistance mutations and inhibitor design. *Biochemistry* **2001**, *40* (31), 9207−14.